Classifying Normal and Abnormal Vascular Tissues using Photoacoustic Signals

Behnaz Pourebrahimi[1], Azza Al-Mahrouki[2], Jason Zalev[3], Joris T. Nofiele [2], Gregory J. Czarnota[2], Michael C. Kolios[1]

Department of Physics, Ryerson University, Toronto, Canada[1]
Imaging Research Department, Sunnybrook Health Sciences Centre, Toronto, Canada[2]
Seno Medical Instruments, San Antonio Texas, USA[3]

mkolios@ryerson.ca

ABSTRACT

In this paper a new method is proposed to classify vascular tissues in the range from normal to different degrees of abnormality based on the Photo-Acoustic (PA) signals generated by different categories of vasculatures. The classification of the vasculatures is achieved based on the statistical features of the photoacoustic radiofrequency (RF) signals such as energy, variance, and entropy in the wavelet domain. A feature vector for each category of vasculature is provided and the distance between feature vectors are computed as the measure of similarity between vasculatures. The distances are mapped in two-dimensional space depicting the proximities of the different categories of the vasculatures. The method proposed in this paper can help both detecting abnormal tissues and monitoring the treatment progress by measuring the similarity between vascular tissues in different stages of treatment. The method is applied to simulated data as well as in vivo data from tumor bearing mice to detect cancer treatment effects.

Keywords: Normal/abnormal vasculature, photoacoustic signals, classification, treatment monitoring, feature extraction

1. INTRODUCTION

Earlier detection of cancer and more effective treatment monitoring methods each offer the opportunity to reduce treatment costs, save lives and improve patient outcomes. Therefore, it is important to develop noninvasive and quantitative tools for tumor diagnosis and treatment monitoring [1]. Biomedical Photo-Acoustic (PA) imaging has developed extensively over the last decade and has many attractive characteristics such as the use of non-ionizing electromagnetic waves, and good resolution and contrast. PA imaging is based on the detection of acoustic waves generated by the absorption of light. When imaging in-vivo, blood has up to six orders of magnitude larger light absorption than the surrounding tissues [2] and therefore the PA pressure waves from the blood tissue dominates the PA signal. Due to this property, PA systems can produce high-contrast images of vascular structures.

Blood vessels are formed in tumors (abnormal tissues) through a process known as angiogenesis. Tumor cells are typically more metabolically active than normal tissues, and therefore require oxygen, nutrients, and must remove their waste. As tumors are structurally abnormal at the cellular, tissue, and vascular levels [3], they contain abnormal, dis-functional, and leaky blood vessels that differentiate them from normal vessels [4]. The vasculature of normal and abnormal tissues can be distinguished by their morphological structures: normal vasculature typically has a highly organized structure. This vascular structure has been modeled to have a narrow range of branching angles at blood vessel bifurcations, while abnormal vasculature has an erratic structure with a wide distribution of branching angles.

It has been theorized [5] [6], and in this work it is assumed that due to dissimilar structures of normal and abnormal tissues, PA signals generated by the two types of tissues have distinguishable features. In [5] [6], the wavelet features of RF-signals from PA signals were classified using a SVM (Support Vector Machine) classifier. In the mentioned work, the classification algorithm only determines whether a vasculature is normal or not. In this paper, we propose a method for monitoring and classification of different categories of normal and abnormal vasculatures/tissues. The method is based on the features extracted from PA signals in the wavelet domain. The distance between features in the two-

Photons Plus Ultrasound: Imaging and Sensing 2013, edited by Alexander A. Oraevsky, Lihong V. Wang,
Proc. of SPIE Vol. 8581, 858141 · © 2013 SPIE · CCC code: 1605-7422/13/$18 · doi: 10.1117/12.2005139

dimensional space monitors the proximities of the vasculature and represents how they are classified. The performance of the method is investigated on data provided by simulation as well as on in-vivo data.

2. MATERIALS AND METHODS

The PA data used in this paper are generated by simulation as well as acquired during in-vivo experiments. A simulation platform has been developed to generate PA data from normal and abnormal tissues [5]. In this platform, the PA signals are generated by a mathematical model for pressure waves from fractal trees that simulate vascular tissues, and are detected by a 128 element transducer array. Details of the simulator can be found in section 2.1 and in [5].

For in vivo experiments, tumor bearing mice are used and RF signals are acquired by scanning the tumor pre and post treatment at given time intervals.

2.1. Simulation of vascular tissues and photoacoustic signals

2.2.1. Fractal tree model

In the literature, many methods are proposed for generating and representing models of vascular structures in tissue [6] [7] [8] [9] [10]. Fractal trees are a way of modeling vascular morphology in tissue based on simple repetitive mathematical rules. Several investigators have used fractal trees to model vascular tissues [9] [10]. A fractal tree is a mathematical structure that is formed by iteratively applying a statistical branching pattern to generate the large scale object. For each iteration, the pattern is specified as a relationship between the parent segment, the left child segment and the right child segment. In this work, we used fractal trees to model normal and abnormal vascular tissues. Each tree is defined by different structural properties such as branching angle distribution, the average vessel length, and the average vessel radius. Branching angle distribution is used as the most significant structural property to distinguish between normal and abnormal vasculature. For instance, a normal tissue is modeled with uniformly distributed branching angles ranging from 25-27°and an abnormal tissue is modeled with branching angles ranging from 25-140° as shown in Figure 1. For a detail description on generating vascular tissues using fractal trees refer to [5].

2.2.2. Photoacoustic signals simulation

When a brief laser pulse illuminates a medium, an initial excess pressure will be created in the medium according to:

$$p_0(x) = \Gamma(x)\mu_a(x)\Phi(x) \qquad (1)$$

where $\mu_a(x)$ is the optical absorption of the medium and $\Phi(x)$ is the energy fluence from the laser. The parameter $\Gamma(\mathrm{x}) = \frac{\beta(\mathrm{x})\mathrm{c}^2(\mathrm{x})}{\mathrm{C_p}(\mathrm{x})}$ is known as the Gruneisen parameter, where $\beta(\mathrm{x})$ is the thermal expansion coefficient, c is the speed of sound and $\mathrm{C_p}(\mathrm{x})$ is the specific heat capacity. If the laser is fired at $\mathrm{t}_0 = 0$, the PA propagation wave at any time and position is determined by:

$$p(x,t) = \frac{\partial}{\partial t}\big(g(x,t) * p_0(x)\big) \qquad (2)$$

where $\mathrm{g}(\mathrm{x},\mathrm{t}) = \frac{1}{\mathrm{c}^2}\frac{\delta(\|\mathrm{x}\|-\mathrm{ct})}{4\pi\|\mathrm{x}\|}$ and $\delta(\mathrm{t})$ is the Dirac impulse function.

To generate a photoacoustic signal for a particular transducer, the PA simulator operates on a fractal tree using cylindrical-segment geometry and simulates PA response from each tree. Each cylindrical vessel segment has a defined start position, end position and vessel diameter to completely specify the fractal tree geometry. To form the PA signal, each cylinder is broken down into many individual PA point sources. The distance of each point source to the transducer is then calculated. Using Eq. (2) the contribution from each PA point source is added to the PA signal. In the simulator, the transducer is configured as a linear array consisting of 128 elements with 0.3*mm* distance between them. Data is captured from the simulator with a sampling rate of 67MHz.

Figure 1: Simulated vascular tissue. For normal tissue, branch angle range varies between 25-27° (a). For abnormal tissue, branch angle range varies between 25-140° (b).

2.2. In-vivo experiments

2.2.1. Cell Culturing and Tumor Induction

Prostate cancer cells (PC3) were cultured in RPMI-1640 media which contained 10% serum and 100 U/mL of Penicillin/Streptomycin. Cells were grown under humidity and at 37°C, 5% CO_2. Confluent cells were harvested using 0.05% Trypsine-EDTA, and were counted using a hemacytometer. CB-17 SCID male mice were injected subcutaneously in one of their hind legs at a concentration of 1X10^6 cells/50µL. The xenograft tumors developed in about a month period, and were treated when the diameters of the tumors reached 7 – 15 mm. Treatment consisted of a novel microbubble mediated treatment [11] that enhances radiation response by acoustical stimulation of the vasculature (that leads to vascular disruption). Microbubbles (MB) were inject through a tail vein catheter, and only the tumor region was subjected to ultrasound (US) exposure. Tumors were exposed to 16 cycles tone burst of 500 kHz frequency with 3 kHz pulse repetition frequency for 5 minutes and with a peak negative acoustic pressure of 570 kpa. Immediately after US treatment, tumors were exposed to radiation. Twenty four hours after treatments animals were sacrificed and tumors were excised for subsequent analyses of the histopathology. Controls included: exposure to US only, to MB only, or no treatment.

2.2.2. Photoacoustic Imaging

Tumors were imaged prior to treatments and 24h after treatments to evaluate any changes in the tumor. The use of photoacoustic imaging modality enabled the monitoring of changes in hemoglobin contents as well as oxygen saturation. Images were acquired using Visual Sonics Vevo LAZR (FUJIFILM Visual Sonics Inc., Toronto, Canada). An LZ-250 transducer was used at a sampling frequency of 21 MHz and a gain of 20 dB. Two different optical excitation wavelengths, 750 nm and 850 nm, were used to generate the photoacoustic images; this was to enable the assessment of the level of change in oxygen saturation. Information from up to 20 individual frames from the middle of each tumor was used in the analyses. A representation of such acquisition is presented in Figure 2.

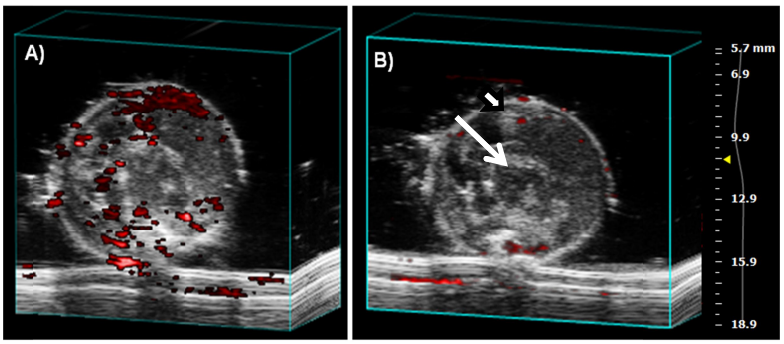

Figure 2. Images of xenograft prostate cancer (PC3) tumors, acquired (A) Before treatment and (B) Twenty four hours after treatment with US/1%MB+8Gy. Photoacoustic images are overlaid on top of the ultrasound B-mode images, block arrow points to the top of the tumor and the long arrow points to the bone of the leg. The yellow arrow on the side scale points to the focus.

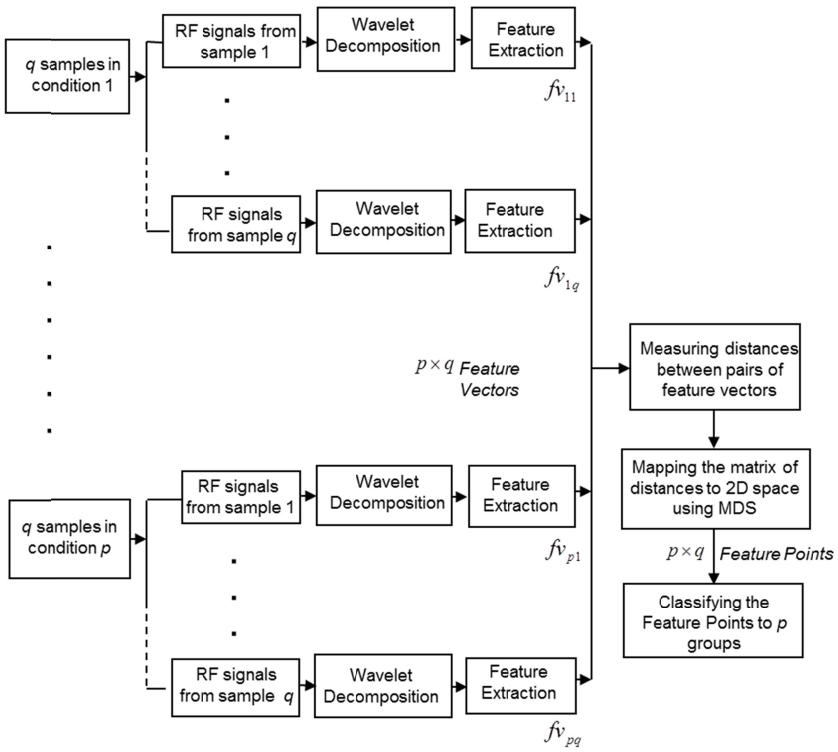

Figure 3: Schematic diagram of the method for the classification of the PA signals.

2.3. Method of classifying and monitoring vascular tissues

The method of classifying and monitoring normal and abnormal vasculature is depicted in Figure 3.

2.3.1. Obtaining RF Signals

The first step is to acquire RF signals through PA imaging. The RF data are provided by simulation of normal and abnormal vasculature (section 2.1) or by in-vivo experiments (section 2.2). We consider p different categories of vasculatures ranging from normal to abnormal. For each vascular category, q samples are obtained (i.e. q samples of each normal or abnormal vasculature). The RF data for each sample contains M signals if the transducer array has M channels.

2.3.2. Extracting Features

From RF data of each sample, a set of discriminative features are computed in the Wavelet domain. Features extracted from each of q samples form a feature vector. In Figure 3, fv_{ij} stands for the feature vector related to sample j in category i.

2.3.3. Statistical Features in the Wavelet Domain

Extracting features in the wavelet domain combines information from both the time and frequency domains. Statistical features such as energy distribution, variance, and entropy are considered to reveal the relevant information required to classify the signals. The features that are selected are the most discriminative for the different categories/conditions. The features are computed for each RF signal / transducer channel and then they are averaged. If $w(n)$ is the wavelet decomposition vector (approximation coefficients vector or detail vector) of a RF signal from a transducer channel, then the features are computed as follows:

- Energy Distribution: The average energy of a signal with the size of N is defined as:

$$\text{energy} = \sum_{n=1}^{N} w(n)^2 \qquad (3)$$

- Variance: The variance is a measure of how far the signal values are spread out from each other.

$$\text{variance} = \frac{1}{N}\sum_{n=1}^{N} (w(n) - \frac{1}{N}\sum_{i=1}^{N} w(i))^2 \qquad (4)$$

- Entropy: Entropy is a statistical measure of randomness that characterizes the smoothness of the signal.

$$e\text{ntropy} = \sum_{n=1}^{N} w(n)^2 \ln(w(n)^2) \qquad (5)$$

The three statistical features are computed for both the low-pass and high-pass sub-band signals at each wavelet scale. Therefore, 3×2 features are obtained at each level (3 features are computed for each of approximation coefficients and detail vectors). Thus, the wavelet decomposition at scale l provides $6 \times l$ features. For instance, in the case of Wavelet decomposition at scale $l = 5$, a feature vector with 30 elements is obtained.

2.3.4. Measuring Feature Distances

For the in-vivo data, it is assumed that for different conditions (e.g. pre-treatment and post-treatment) the tumor properties change due to change in vascular structure that are caused by the treatment, or due to the changes in vascular structure related to tumor growth. Therefore, we expect the PA signals obtained to differ for the different conditions. This should be reflected also in the features that are derived from the PA signals. Based on this assumption, the proximity between feature vectors in different conditions signifies the changes in tissue due to the treatment. Feature vectors further apart would be indicative of greater change in the tumor tissue vasculature. The distance between feature vectors is considered as a measure of the similarity between them. The Euclidean distance is used to compute the distance between each pair of the vectors. A matrix of distances is provided in this step. Having $p \times q$ feature vectors, a matrix of distances with size of $(p \times q)^2$ is obtained.

2.3.5. Monitoring and classifying the samples

In order to visualize the distances between feature vectors, a Multi-Dimensional Scaling (MDS) analysis [12] is used to map the distance matrix to a two or three-dimensional space. The MDS provides a visual representation of the pattern of similarities or dissimilarities among the samples. Each sample is represented by a point in a multidimensional space. The points are located in this space so that the distances between them are strongly related to the similarity of the samples. Two similar samples are represented by two points that are close together, and two dissimilar samples are represented by two points that are far apart. By applying MDS to the matrix of distances, $p \times q$ points in 2-dimensional space, each corresponding to one sample, are obtained. We call these points as the *'feature points'*. By mapping feature points in two-dimensional space, we monitor the samples and their similarities. Samples belonged to the same condition are classified in one group.

3. RESULTS

The proposed method was applied to two sets of data. One simulated and another obtained from in-vivo experiment on tumor bearing mice.

3.1. Simulated data

For the first set of data, four groups of vasculatures were generated ranging from normal to abnormal. The level of normality (or abnormality) is defined by the branching angles in the simulated fractal tree vasculature. A normal vasculature is considered to have branching angles between the range of 25-27° and a vasculature with branching angles in the range 25-140° is considered to be abnormal. Two other groups with branching angles of 25-40° and 25-80° were considered in the range between normal and abnormal. Five samples from each group were taken. PA signals from each

sample were simulated and then a feature vector in wavelet domain was extracted for each sample. The distance between feature vectors were computed and mapped to a two-dimensional space using MDS.
Figure 4 plots the samples of four groups of vasculatures in the two-dimensional space. Each symbol in the figure represents one group of vasculatures and similar symbols with the same color show samples that are known to be in the same group. The distance between sample points shows their similarity. As seen from the figure, the samples of the same group are located closer to each other and the groups with more similar structures (more similar branching angles) are next to each other. The four groups of vasculatures are arranged in the order of their similarity. As MDS is a method for visualizing proximities between samples, the axis show relative distance between feature points in two-dimensional space and the numbers are dimensionless quantities.

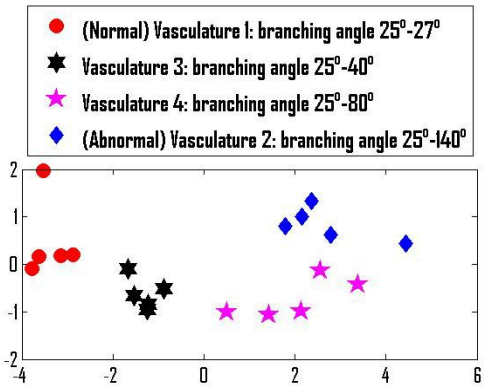

Figure 4: Monitoring 4 groups of vasculatures in two-dimensional space

3.2. In-vivo experiments

The algorithm was then applied to in-vivo data from tumor bearing mice, as described in section 2.2. Two cases were considered: control and treated. PA signals were acquired before and after 24 hours for both control (untreated) and treated mice. The frames obtained through scanning the tumor were considered as the samples of the particular condition. For each mouse, we selected the frames, which contain tumor planes with the largest tumor physical dimensions (typically in the middle of the tumor). The algorithm was applied on the beamformed RF data of each frame within a region of interest that enclosed only tumor tissue. The aim was to monitor and classify the tumor frames pre and post treatment, for both the control mouse (no ultrasound or radiation treatment but with the mouse exposed to the same set-up conditions) and the treated mouse (active ultrasound and radiation treatment).

Figures 5(a) and 5(b) show the results of applying the algorithm on the two mice. Mouse1 was the control and Mouse2 was the treated mouse. For each mouse in each condition of pre and post treatment, 15 frames (samples) were analyzed. We expect to see greater similarity between the frames of pre-treatment and post treatment for the control mouse. For the treated mouse, we expect to observe greater dissimilarity between pre and post-treatment frames (provided the treatment was effective). As the results show, the pre and post-treatment frames of control mouse are similar and cannot be distinguished. In the treated mouse, we observe pre-treatment and post-treatment frames can be classified into two groups. For instance, a clustering algorithm (such as Fuzzy c-Means [13]) can be applied on sample points in Figure 5(b) and divide the samples into two groups of pre and post treatment. This clustering cannot distinguish between the samples in Figure 5(a). In this paper, we do not discuss such clustering algorithms.

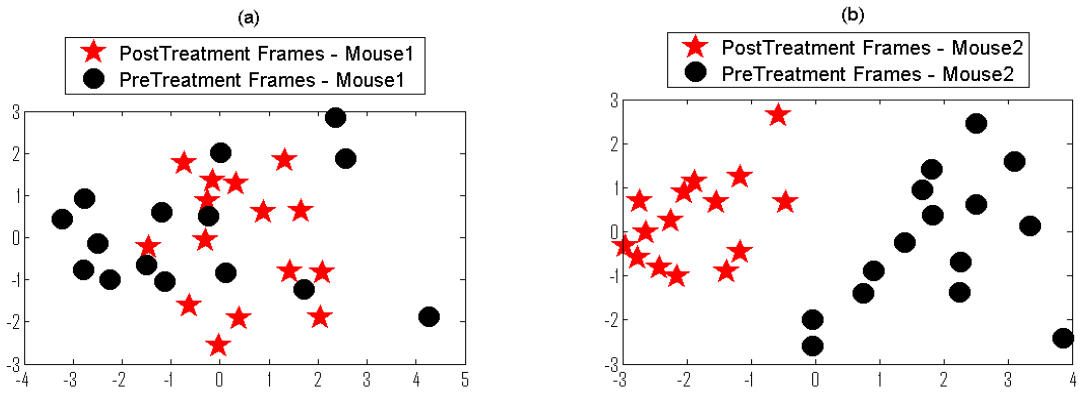

Figure 5: Monitoring pre-treatment and post-treatment frames in two mice: (a) control, and (b) treated.

4. CONCLUSIONS

In summary, a novel method is proposed to monitor treatment effects by classifying normal and abnormal vasculature and visualizing a cancerous tumour pre and post treatment through the analysis of photoacoustic signals. The aim is to classify different levels of vascular abnormality in the treated tumor.

The method was applied on two sets of data: one from simulations and another from in-vivo experiment. Photoacoustic signals were obtained by a mathematical model (the simulation) or by scanning a tumor pre and post treatment (the in-vivo experiment). For each set of photoacoustic data, a set of discriminative features were computed as a feature vector. The distances between feature vectors in different conditions were measured to detect the proximities in the vasculature/tissue samples. To visualize the proximities, the distances were mapped in a two-dimensional space. In the final map, each point represents a sample of vasculature or tumor frame in a particular condition. The distance between points shows how similar the samples are. Smaller distances represent more similarity and larger distances represent more dissimilarity. Using this method, the treatment effect can be studied by monitoring the tumor tissue samples before and after treatment and investigating the samples proximities.

REFRENCES

[1] Xiang, Liang Zhong and Zhou, Fei Fan, "Photoacoustic Imaging Application in Tumor Diagnosis and Treatment Monitoring," Key Engineering Materials,1100-1104 (2007).

[2] Yao, J. and Wang, L. V., "Photoacoustic tomography: fundamentals, advances and prospects," Contrast Media Mol Imaging., 6(5), 332-345 (2011).

[3] Papetti, Michael and Herman,Ira M., "Mechanisms of normal and tumor-derived angiogenesis.," Americal Journal of Cell Physiology, 947-970 (2001).

[4] Jain, R. K., "Taming Vessels to Treat Cancer," Scientic American, 56-63(2008).

[5] Zalev, Jason, "Detection and monitoring for cancer and abnormal vasculature by photoacoustic signal characterization of structural morphology," Thesis and Dissertations, Ryerson University, (2010).

[6] Zalev, Jason and Kolios, Michael C., "Detecting abnormal vasculature from photoacoustic signals using wavelet-packet features," in Proc. SPIE 7899, Photons Plus Ultrasound: Imaging and Sensing , (2011).

[7] Herrero, M. A., Kohn, A. and Peres-Pomarez, J. M., "Modelling Vascular Morphogenesis: Current Views on Blood Vessels Development," Mathematical Models and Methods in Applied Sciences , vol. 19, 1483–1537 (2009).

[8] Wang, L., Bhalerao, A. and Wilson, R., "Analysis of Retinal Vasculature Using a Multiresolution Hermite Model," IEEE Trans Medical Imaging, 26(2), 137–152(2007).

[9] Karshafian. Raffi., "Modelling the structure of the tumour vasculature and its effect on Doppler ultrasound signals," master's thesis, University of Toronto,(2001).

[10] Zamir, M., "Arterial branching within the confines of fractal L-system formalism," General Physiology 118(3), 267–275, (2001).

[11] Czarnota, Gregory J., Karshafian, Raffi, Burns, Peter N., Wong, Shun, Al Mahrouki, Azza, Lee, Justin W., Caissie, Amanda, Tran, William, Kim, Christina, Furukawa, Melissa, Wong, Emily and Giles, Anoja, "Tumor radiation response enhancement by acoustical stimulation of the vasculature," the National Academy of Sciences , 109(30) E2033 (2012).

[12] Steyvers, M. , "Multidimensional scaling," Encyclopedia of cognitive science, (2002).

[13] Bezdek, James C., Ehrlich, Robert and Full, William, "FCM: The fuzzy c-means clustering algorithm," Computers & Geosciences, 191–203(1984).

[14] Noble J.A., "Ultrasound image segmentation and tissue characterization,"Proc Inst Mech Eng H., 307-316 (2010).